ELSEVIER

Development of a Two-Dimensional Liquid Species Concentration Measurement Technique Based on Absorptiometry

J. Mihailovic
C. Beckermann
Department of Mechanical Engineering, The University of Iowa, Iowa City, Iowa

■ A nonintrusive optical technique is developed for species concentration measurements in liquid solutions. The technique is based on absorptiometry and uses digital image analysis to measure quantitatively two-dimensional concentration distributions. The apparatus and calibration procedures are described in detail, and the accuracy and resolution are established in uniform concentration and one-dimensional diffusion experiments. The technique is then applied to measure concentration fields during double-diffusive convection in a Hele-Shaw cell, and good agreement with numerical predictions is obtained. The limitations and possible enhancements of the technique are briefly discussed.

Keywords: *absorptiometry, optical techniques, binary diffusion, double-diffusive convection*

INTRODUCTION

The measurement of species concentration distributions in liquids is of interest in numerous coupled heat and mass transfer systems, such as crystal growth and solidification of melts and solutions. Most recently, attention has been devoted to the development of nonintrusive optical techniques, making use of refractometry [1, 2], phase contrast [3], interferometry [4, 5], polarigraphy [6, 7], and absorptiometry [8–11]. Often, the systems are characterized by simultaneous variations in species concentration and temperature. This leads to considerable difficulties [3, 5] in separating their combined effect on the index of refraction, which is the optical property of interest in refractometric, phase contrast, and interferometric methods. Polarigraphic and absorptiometric techniques, on the other hand, are rather insensitive to temperature, making an independent measurement of species concentration possible. The advantages of polarigraphy are discussed in detail by Paul and Bergman [7]. One major disadvantage of polarigraphy is that it is limited to species having optical rotary power (e.g., sucrose). Absorptiometry is, of course, limited to species having a spectrum where the absorbance shows sufficient sensitivity to concentration at the wavelength of the light source (e.g., laser) used. Nonetheless, the wide availability of lasers covering a broad range of wavelengths makes this technique suitable for numerous liquid solutions. Typically, absorptiometric techniques rely on a (narrow or expanded) test beam traversing a test cell containing the liquid. As such, they provide a measurement of concentration that is averaged along the path of the beam. In addition, in a nonuniform concentration/temperature field, the beam is subject to refraction, posing serious problems near the cell boundaries and other interfaces (this appears to be less of a problem in polarigraphy due to forward scattering [7]).

Absorptiometry was first used by Kazmierczak and Poulikakos [8] and later by Gau and Wu [9] to measure concentrations of aqueous cupric sulfate solutions using a He-Ne laser. Gau and Wu also reported on concentration measurements in a flow situation involving double-diffusive convection. Both systems [8, 9] relied on a narrow laser beam and a simple power meter to measure the depth-averaged concentration over a small circular area of the test cell. By traversing the optical system, steady-state species concentration profiles were obtained. However, in a transient situation the above systems would provide only point measurements and it would be nearly impossible to obtain two-dimensional concentration field data. The more advanced measurement systems developed by Körber et al. [10] and Kourosh et al. [11] are geared toward cryobiological applications and are concerned with concentration distributions on a microscopic scale (e.g., within biological cells) in a purely diffusive environment. There appears to be a continued need to further develop absorption-based species concentration measurement techniques for use with liquid solutions.

The objective of the present study is to employ absorptiometry to measure instantaneously two-dimensional species concentration distributions. Use is made of an expanded, collimated laser beam that is imaged on a CCD

Address correspondence to Professor C. Beckermann, Department of Mechanical Engineering, The University of Iowa, 2129 Engineering Building, Iowa City, IA 52242-1527.

Experimental Thermal and Fluid Science 1995; 10:113–123

655 Avenue of the Americas, New York, NY 10010
0894-1777/95/$9.50
SSDI 0894-1777(94)00069-K

camera for digital analysis of the light intensity field. This article describes in detail the procedures necessary to obtain quantitative concentration data. In addition, the developed absorptiometric system is applied to a complex two-layer double-diffusive convection experiment and the measured species concentrations are compared with the results of a numerical simulation [12].

EXPERIMENTAL TECHNIQUE

The present measurement technique is based on the Lambert–Beer law, which can be written as

$$I = I_0 e^{-\alpha C}, \tag{1}$$

where I_0 and I are the intensities of the light incident on and emerging from the solution, respectively, α is the absorption coefficient, and C is the concentration of the solution. Equation (1) is valid on a spectral basis, and α is a function of the type of solution used and the wavelength of the light and increases linearly with the optical path length. Clearly, the measurement of concentration requires the knowledge of α and the ratio I/I_0. The sensitivity depends on the absorption coefficient α and can be maximized by proper matching of the solution type, laser wavelength, and test cell thickness. Once this selection is made, α can be determined in a separate calibration procedure described below in more detail. Through the local measurement of I/I_0, Eq. (1) can then be applied at each point on a two-dimensional plane normal to the light beam to determine the concentration field.

EXPERIMENTAL APPARATUS

A schematic of the experimental setup is shown in Fig. 1*a*. The light source consists of a Coherent Innova 90 argon-ion laser that was operated at both $\lambda = 488$ nm (blue light) and $\lambda = 514.5$ nm (green light). The laser beam passes through a Newport Model 900 spatial filter and is expanded and collimated to a diameter of about 100 mm by a system of lenses. A part of the collimated beam (i.e., the test beam) then passes through the test cell, while another part is used as a reference beam and passes over the test cell. Both beams are incident on a rotating diffusive glass screen located directly adjacent to the back of the test cell. The need for the reference beam and the rotating glass screen is discussed below. The light intensity distribution on the screen is recorded with a Photometrics 200 CCD camera system connected to a Macintosh II computer. The CCD imager contains a rectangular matrix of 384 × 576 pixels with 4096 gray levels per pixel. The image of the test section occupied about 240 × 240 pixels. In all experiments, the average value of the incident light intensity, I_0, was adjusted to be in the upper gray level range, that is, at about 3500. This maximizes the range of measurable concentrations, since I_0 is always greater than I. The incident light intensity varied by up to ± 300 gray levels from the mean over the test section. These variations directly reduce the range of the concentration measurements and should therefore be minimized. They do not affect the accuracy of the technique, because Eq. (1) is applied on a pixel-by-pixel basis. In no case should the measured gray level fall below about 100, because of the dark-field noise of the CCD camera. In some of the experiments the CCD camera was replaced with a Nikon

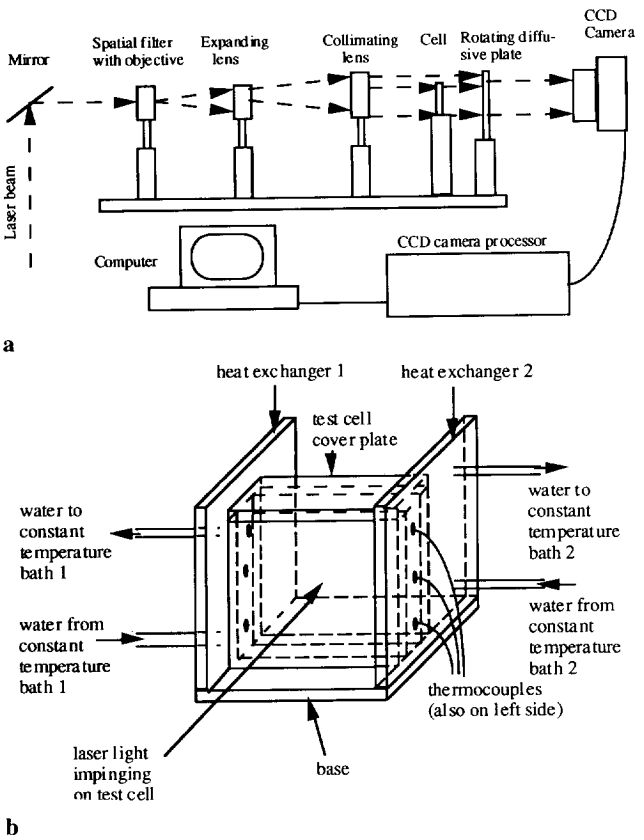

Figure 1. Schematic of the experimental setup. (*a*) Optical system; (*b*) Test cell for the double-diffusive experiment.

FM2 photo camera for qualitative flow visualization.

The test cell, illustrated in Fig. 1*b*, consists of two copper heat exchangers forming the two vertical side walls, 6.5-mm-thick × 51.3-mm-square Pyrex glass plates as the transparent front and back walls, a 12.7-mm-thick phenolic base, and a 1.6-mm-thick acrylic top cover. The gap between the two glass plates, or the depth of the solution along the light beam, was chosen to be only 1.6 mm. The test cell thus resembles a square Hele-Shaw cell with heating/cooling from the side walls and approximately adiabatic top and bottom boundaries. A Hele-Shaw cell lends itself especially well as a laboratory apparatus to study two-dimensional diffusion/convection patterns. There exists a direct mathematical similarity between two-dimensional flow in a porous medium and laminar flow in a Hele-Shaw cell [13]; both are governed by Darcy's law. Because of the small thickness of the liquid layer between the glass walls, refraction of the light beam passing through the test cell is minimized. Sealing and accurate positioning of the glass plates is important, and this was accomplished by attaching small acrylic strips to the outer edges. Unfortunately, the strips blocked some of the view of the test section, making the CCD and photographic images slightly smaller than the inside dimensions of the cell (see figures). The heat exchangers were made of 19-mm-thick copper blocks with multipass internally milled channels through which water from individual Haake N3 refrigerated constant-temperature baths was circulated. Three thermocouples embedded near the sur-

face of each heat exchanger indicated that the side walls were isothermal to within ± 0.1°C of the desired hot and cold wall temperatures. Except during the optical measurements, the whole apparatus was encased in 5-cm-thick foam insulation. To further reduce the thermal interaction with the environment, the mean cell temperature was maintained at exactly room temperature and the temperature difference between the heat exchangers was kept below 5°C. During the isothermal experiments, described in more detail below, the vertical side walls were simply made of acrylic (instead of copper) and no insulation was used.

An aqueous solution of $KMnO_4$ was chosen as the binary liquid, mainly because it provides good absorption characteristics for the relatively thin liquid layer and the argon-ion laser wavelengths considered here. The thermophysical properties of aqueous $KMnO_4$ solutions are well established [5, 14, 15]. The maximum concentration of the solution in the experiments was only 3×10^{-3} weight fraction $KMnO_4$, enabling the use of pure water values for properties such as the thermal diffusivity, specific heat, and viscosity of the solution. The solutions were prepared using a Sartorius 2462 laboratory balance with an accuracy of 0.0001 g, degassed and distilled water, and laboratory grade $KMnO_4$. All solutions were prepared by diluting a "mother" solution of the maximum concentration. An error analysis [16] indicated an uncertainty of about 10^{-5} weight fraction $KMnO_4$ in the concentrations of the prepared solutions.

DATA REDUCTION PROCEDURES

Considerable effort was undertaken to ensure consistent and accurate CCD camera light intensity measurements. The conversion of the intensity data to concentrations is discussed in the next section. There are mainly two effects that hamper the intensity measurements in the present system: (1) the well-known speckle effect and (2) laser light intensity fluctuations. To investigate these effects, the test cell was filled with distilled water and, for each case discussed below, two consecutive CCD images were taken, about 15 s apart. The measured intensities (ranging from 0 to 4095) of the two images were then ratioed pixel by pixel. Figures 2*a*–2*c* each show an arbitrarily selected column of such pixel intensity ratios.

Figure 2*a* illustrates the speckle effect in full power, when the glass screen is not rotating. Essentially, the intensities fluctuate wildly and are not reproducible from one exposure to another. Figure 2*b* shows a considerable reduction in the speckle effect for a rotating glass screen. The glass screen was rotated at about 90 rpm, which serves to integrate the diffraction patterns due to the screen structure over the exposure time (here about 1.0–1.5 s). Although the rotational speed varied substantially over the test section, the reduction in the speckle effect appears to be relatively uniform (see Fig. 2*b*). Nonetheless, an increase in the rotational speed would further decrease the speckle effect, particularly if shorter exposure times were used. A further reduction in the noise can be achieved by employing a straightforward smoothing procedure, the results of which are illustrated in Fig. 2*c*. Here, a pixel intensity is replaced by the arithmetic average of the 25 intensities of the pixel and its immediate 24 neighbors (in all directions). Other schemes

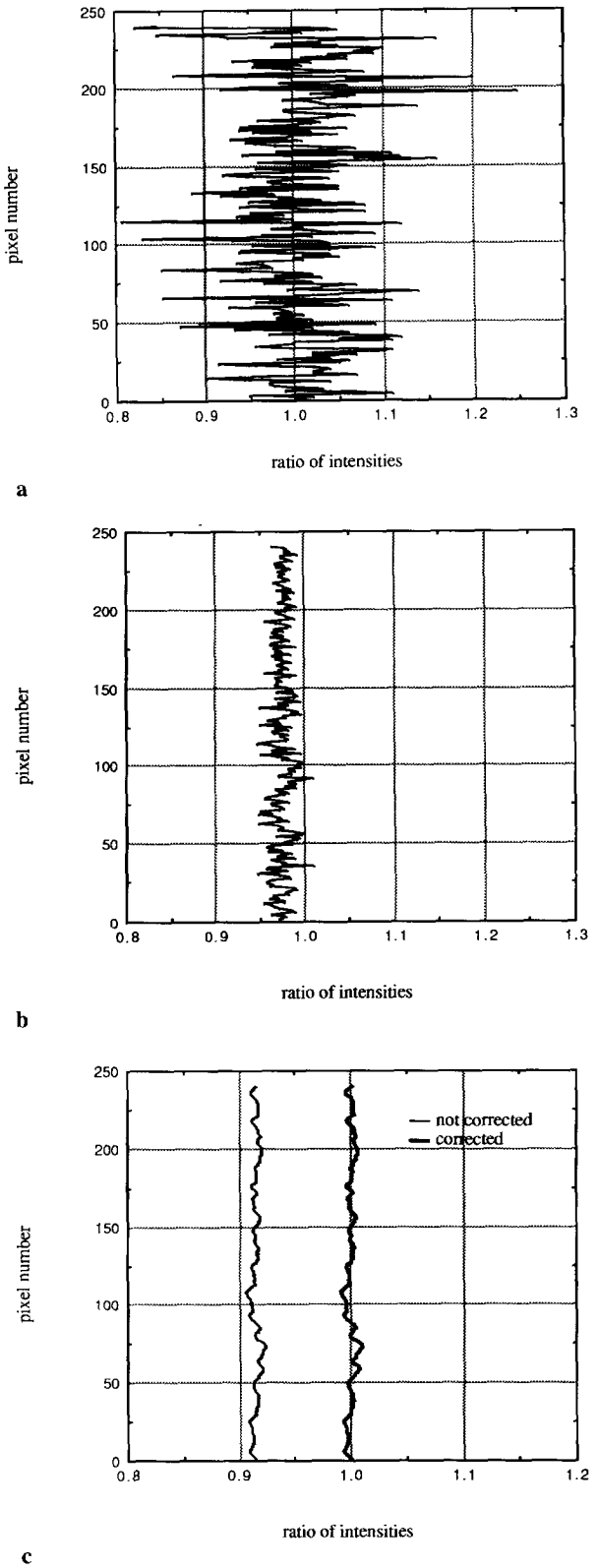

Figure 2. Columns of pixel intensity ratios of two consecutive exposures. (*a*) No rotation of screen, no smoothing, no intensity correction. (*b*) Reduction of the speckle effect due to screen rotation. (*c*) Effect of smoothing on the pixel intensity ratios without (thin line) and with (thick line) light intensity correction.

are possible. For the 240 × 240 pixels used for the test section, this procedure can be viewed as a reasonable compromise between noise reduction and loss of spatial resolution. With the averaging, the spatial resolution was estimated to be at least 1 mm over a length of 50 mm. This resolution could be much improved by using a different CCD chip with more pixels or by focusing on a particular region of the test section. The remaining noise represents less than 1% of the intensity ratio.

It is also apparent from Fig. 2*c* that the ratio of the intensities is, on the average, not equal to unity. This can be attributed to changes in the laser power during the time interval between the two exposures. In measuring concentration, this would be a serious problem, as changes in the light intensity due to laser power fluctuations and changing light absorption in the cell cannot be easily separated. For this reason, a simple correction procedure was developed that uses the reference beam passing over the test cell. It is assumed that the laser light intensity fluctuations at each pixel are linearly related. Then the ratio of the light intensities of the reference beam between two exposures is used as a correction factor that multiplies each pixel value in the test section. Figure 2*c* illustrates that the result is satisfactory. It was found that this correction procedure works well for the relatively large laser power drifts that can occur over a period of hours. Apparently, the intensity correction procedure is accurate to within the remaining noise in the system. A more detailed analysis of the total optical system uncertainty is given by Mihailovic [16]. Estimates of the resulting uncertainty in the measured concentrations are provided below.

CALIBRATION PROCEDURE

The absorption coefficient in Eq. (1) was found by filling the test cell with solutions of known concentration and measuring the resulting light intensity, I. Equation (1) was solved for α, and I_0 represents the light intensity measured for pure water ($C = 0$). In this way, the absorption coefficient was determined for each pixel, that is, each location on the image plane. The arithmetic average of all pixel absorption coefficients is plotted in Fig. 3 as a function of concentration for the green and blue laser light. It can be seen that the mean absorption coefficient is different for the two laser wavelengths and that the wavelengths are characterized by different sensitivities and ranges where the Lambert–Beer law is applicable (i.e., the absorption coefficient is independent of concentration). The best fits of α in Fig. 3 do not include the data that are obviously outside the range of applicability. The deviations from the best fits at very small concentrations can mainly be attributed to errors in solution preparation and the increased relative importance of noise when I approaches I_0 [16]. The blue light was used in all subsequent experiments, because it gives a constant absorption coefficient up to the maximum concentration of interest in this study. However, the above results indicate that it is possible to tailor the sensitivity of the present method by choosing different wavelengths and that it may be useful to employ more than one wavelength to increase the range of sensitivity.

The calibration procedure also showed that the local (pixel) absorption coefficients varied by up to ±5% from the mean over the test section [16]. However, this was not a random error but could be attributed to nonuniformities in the gap thickness of the test cell. This systematic error was eliminated by employing the local (pixel) values of the absorption coefficient instead of the mean α shown in Fig. 3 in the concentration measurements.

RESULTS AND DISCUSSION

Preliminary experiments were conducted to ascertain the accuracy of the present technique for isothermal situations. These include measurements of uniform concentrations and of one-dimensional concentration distributions. Then the technique was applied to double-diffusive convection involving unsteady, two-dimensional temperature and concentration variations and a flowing liquid.

Preliminary Experiments

Figure 4 shows a comparison between actual (nominal) and measured concentrations for an isothermal test cell filled with a uniform concentration solution. The agree-

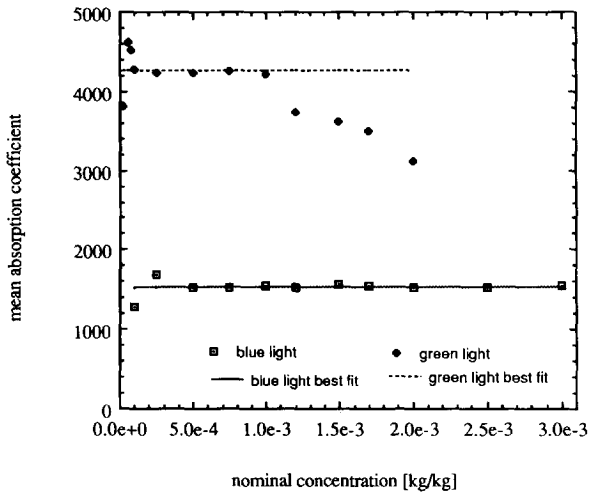

Figure 3. Mean absorption coefficient as a function of concentration for blue and green laser light.

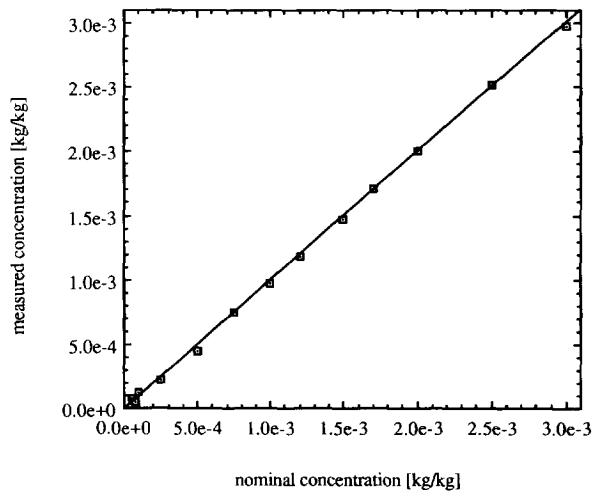

Figure 4. Comparison of measured and nominal concentrations for a uniform concentration solution.

ment is very good, with the discrepancies falling within the estimated experimental uncertainty of about $\pm 3 \times 10^{-5}$ weight fraction $KMnO_4$ [16]. These results indicate that with the present technique it is possible to accurately measure uniform species concentrations over a concentration range spanning more than an order of magnitude in the weight fraction.

One-dimensional isothermal diffusion experiments were conducted by carefully introducing a layer of pure water above a layer of a concentration of 1.7×10^{-3} weight fraction $KMnO_4$. All measured concentrations were horizontally averaged over each pixel row. The experiment was numerically simulated by solving the one-dimensional unsteady diffusion equation. The accuracy of the numerical results was confirmed through comparisons with an available analytical solution for semi-infinite layers and a step change in the initial concentration at the interface between the two layers. Details can be found elsewhere [16]. Because in the experiments the initial interface between the two layers was not entirely sharp, the measured initial concentration distribution was used as an input in the numerical simulation.

Figure 5*a* shows a comparison of the measured and predicted concentration profiles at 8 h 50 min into the experiment. The agreement between the two profiles is good. In addition to the experimental uncertainty, some discrepancies can be attributed to (1) uncertainties in the value of the diffusion coefficient and (2) the fact that the initial concentration distribution was not entirely horizontally uniform. An additional check of the measurements can be achieved by considering overall species conservation in the test cell. Figure 5*b* shows measured concentrations as a function of time averaged over the upper portion, the lower portion, and the entire test cell. It can be seen that the results are consistent with the expectations over the experimental period of 22 h.

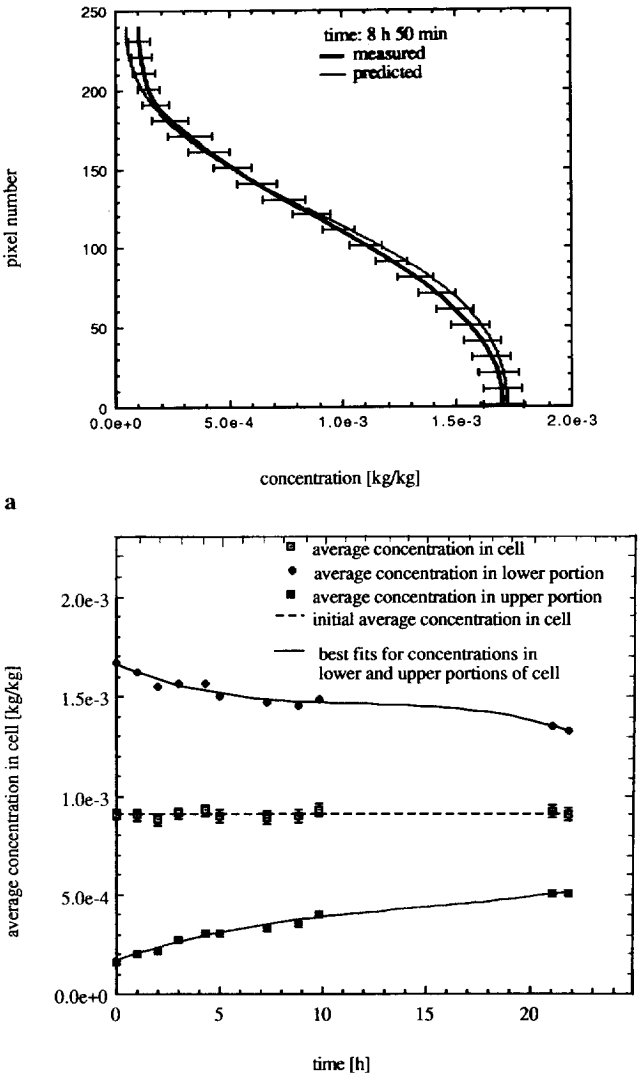

Figure 5. Results of the one-dimensional isothermal diffusion experiment. (*a*) Comparison of measured and predicted concentration profiles at 8 h 50 min. (*b*) Evolution of average concentrations in the test cell.

Double-Diffusive Experiment

As in the one-dimensional diffusion experiment, the double-diffusive system initially consists of two isothermal, horizontal liquid layers of different concentration. At $t = 0$, the layers are destabilized by lateral heating/cooling. Recirculating liquid motion within each layer is thermally driven. Owing to solute transport across the interface between the layers (i.e., the double-diffusive interface), the concentration difference between the layers decreases with time, the interface becomes more vertical, and ultimately the layered structure breaks down and the liquid mixes vigorously. Such two-dimensional, double-diffusive convection in a Hele-Shaw cell is analyzed numerically in [12], which also contains a detailed description of the system dynamics. Here, we attempt a direct comparison between predictions and measurements.

In the analysis of [12], it is assumed that the flow is governed by Darcy's law, that local thermal equilibrium exists between the front and back glass walls and the solution (i.e., the heat transfer in the glass walls is included in the analysis), and that the Boussinesq approximation applies. The dimensionless governing parameters are the Darcy–Rayleigh number, Ra; the Lewis number, Le; the stability number, N; and the thermal capacitance ratio, σ (for a square cavity). The governing transport equations for heat and solute are solved using the flux-corrected transport (FCT) scheme, which reduces the diffusive error to sixth order; an explicit two-time-step approach, which maintains second-order time accuracy; and a 101×101 uniform grid. Other details can be found in [12].

In the experiment, the initial concentration difference between the two layers was 1.65×10^{-3} weight fraction $KMnO_4$, and the temperature difference between the hot and cold side walls was 5°C. This corresponds to the following values of the governing parameters: Ra = 50.8, Le = 438.5, $N = 1.0$, $\sigma = 4.11$ [12]. There is an uncertainty of about 5% in the values of these parameters because of uncertainties in the values of the thermophysical properties, the temperatures, the initial concentrations, and the test cell gap width.

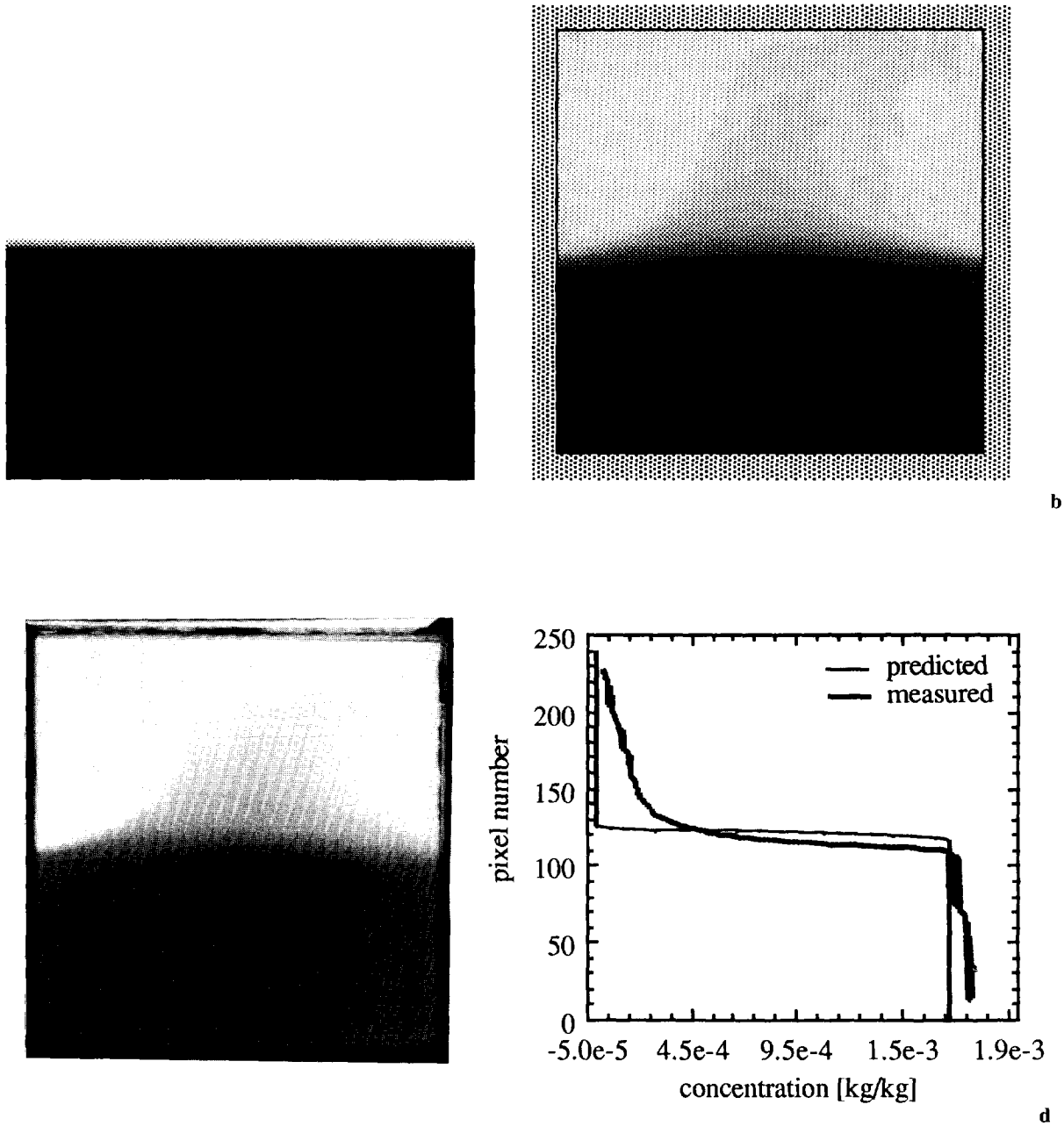

Figure 6. Results of the double-diffusive experiment at $t = 0$. (*a*) Predicted concentration field. (*b*) Measured concentration field. (*c*) Photograph. (*d*) Comparison of measured and predicted vertical concentration profiles at the cell midsection.

Figures 6–10 show representative results at $t = 0$, 29, 144, 230, and 274 min into the experiment, respectively. At $t = 296$ min, layer mixing initiated and the experiment was stopped. In each figure, panels *a* and *b* show the numerically predicted and measured species concentration fields, respectively, with the gray level indicating the concentration value. Panels *c* show a regular photograph of the test section. The photographs and the CCD camera pictures were taken at the same nominal times but in different experiments, so some differences exist. Panels *a*, *b*, and *c* can be compared only qualitatively (although each gray level in panels *a* and *b* does correspond to a unique concentration value). Panel *d* in each figure shows a quantitative comparison between measured and numerically predicted concentration profiles at various locations, as indicated in the figure captions.

Figure 6 shows the initial concentration distribution at $t = 0$ min, just before the heating/cooling was initiated. It can be seen that the initial concentration distribution in the experiments is not entirely steplike, which can be attributed to the way the pure water layer was introduced above the $KMnO_4$ solution. Although it would have been

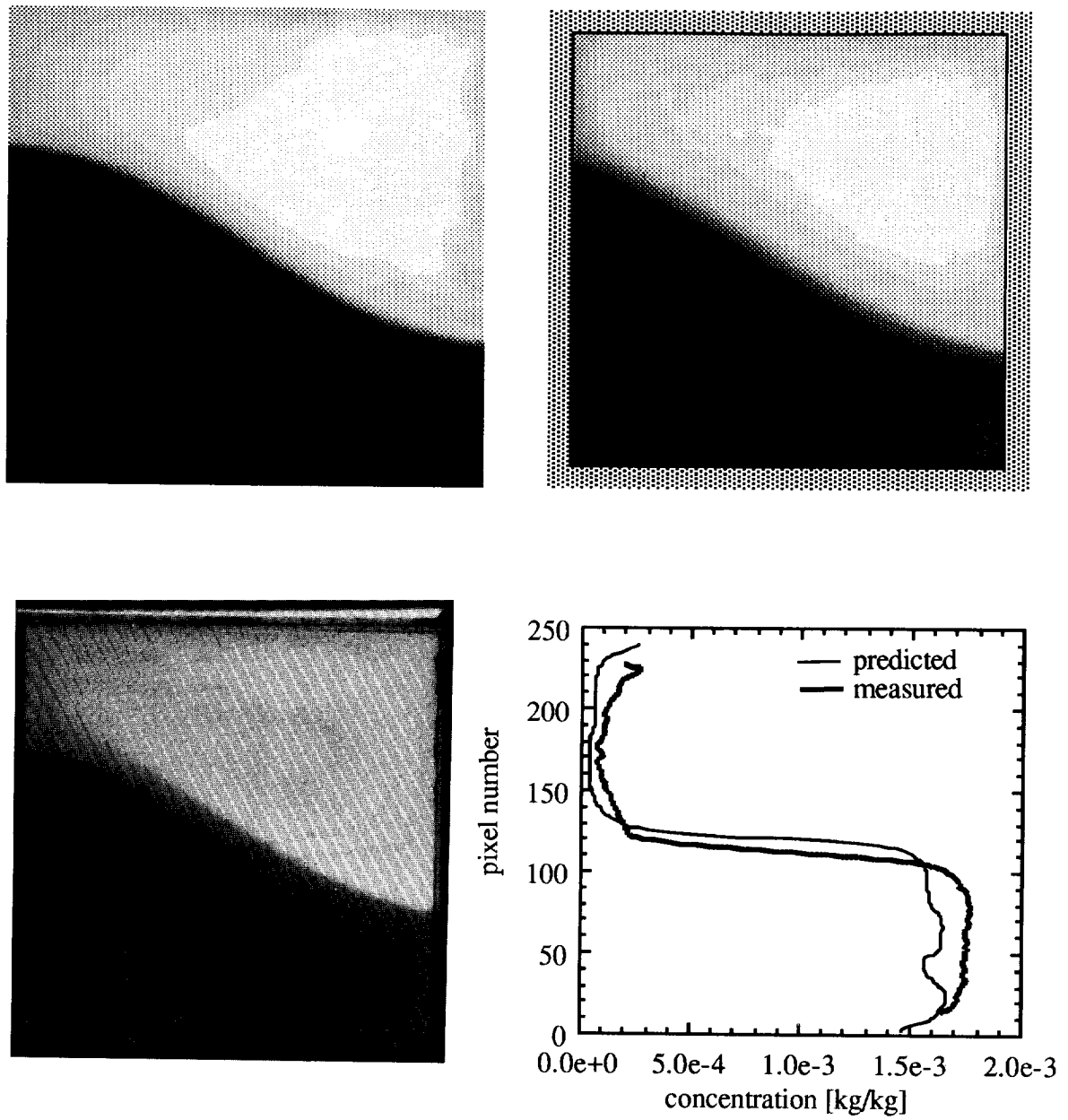

Figure 7. Results of the double-diffusive experiment at $t = 29$ min. (*a*) Predicted concentration field. (*b*) Measured concentration field. (*c*) Photograph. (*d*) Comparison of measured and predicted vertical concentration profiles at the cell midsection.

possible to use the measured concentration field as an initial condition in the numerical simulation (instead of the step change in Fig. 6*a*), the initial differences are not expected to have a large influence on the overall flow structure at later times.

Figures 7–10 generally show good agreement between the measured and predicted concentrations for $t > 0$. The location and shape of the double-diffusive interface between the two layers are very sensitive to the system parameters and the heat and mass transfer phenomena within the layers. Nonetheless, both the shape of the concentration profiles and the concentration values appear to be well predicted. In particular, panels *d* show good agreement in the measured and predicted magnitudes of the steep concentration gradient across the double-diffusive interface. To our best knowledge, these figures represent the first direct comparison between measured and numerically predicted two-dimensional concentration fields in double-diffusive convection. One possible reason for some of the discrepancies is the large unsteadiness in the flow. This is illustrated in Fig. 11, where the predicted concentration history at two points in the layers is plotted (this figure is from [12] and is for somewhat different governing parameters). Before layer turnover,

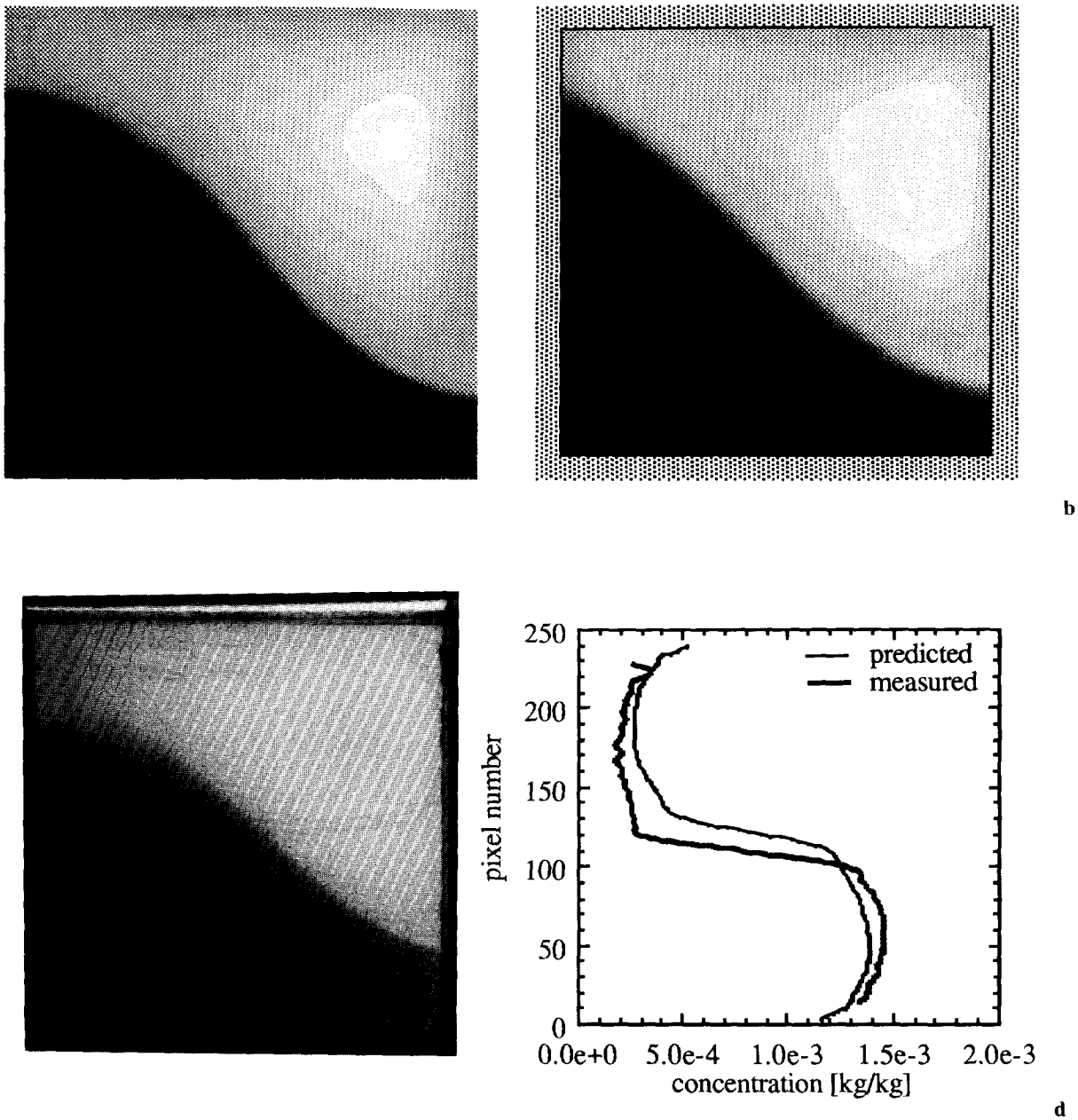

Figure 8. Results of the double-diffusive experiment at t = 2 h 24 min. (*a*) Predicted concentration field. (*b*) Measured concentration field. (*c*) Photograph. (*d*) Comparison of measured and predicted vertical concentration profiles at the cell midsection.

the concentrations "randomly" fluctuate by up to 10% from the mean. These fluctuations correspond to small-scale structures in the flow and concentration fields [12] that are nearly impossible to match between different experiments and the simulation. A more thorough investigation into these fluctuations is not attempted here. Other discrepancies may be attributed to inaccurately modeled initial (see above) and boundary conditions, such as the neglect of heat transfer to and from the insulated front, back, top, and bottom walls of the test cell, uncertainties associated with the thermophysical properties, and possible numerical inaccuracies. The effect of these uncertainties on the predicted concentrations is difficult to quantify but can be expected to cause less than a 10–20% difference between the measured and predicted results.

SUMMARY AND CONCLUSIONS

A two-dimensional absorptiometric technique has been developed to instantaneously measure species concentration fields in liquid solutions. The apparatus and procedures necessary for obtaining quantitative concentration

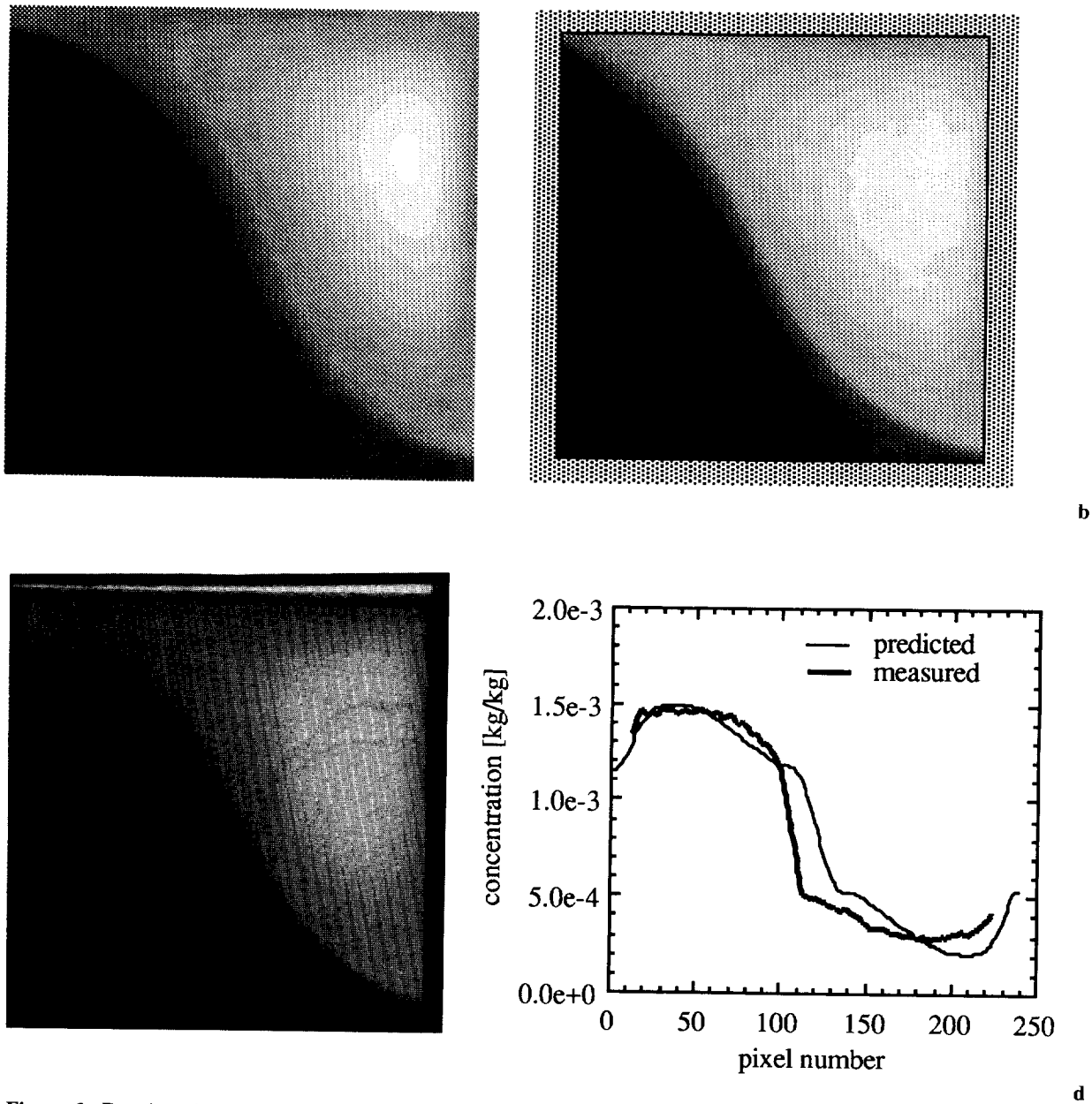

Figure 9. Results of the double-diffusive experiment at $t = 3$ h 50 min. (*a*) Predicted concentration field. (*b*) Measured concentration field. (*c*) Photograph. (*d*) Comparison of measured and predicted horizontal concentration profiles at the cell midsection.

data have been reported in detail. The accuracy and resolution of the technique have been established through preliminary experiments involving uniform concentration solutions and one-dimensional diffusion in a relatively thin test cell that minimizes refraction. It is emphasized that the sensitivity of the technique can be adjusted by matching the light wavelength and test cell thickness to the type of solution and concentration range to be measured. The double-diffusive experiment has demonstrated the utility of quantitative absorptiometry in complex situations involving convection and heat transfer. Comparisons with a numerical simulation have shown good overall agreement, although several aspects of the highly unsteady double-diffusive convection phenomena remain to be investigated.

RECOMMENDATIONS AND FUTURE RESEARCH

As in most optical methods, refraction of the test beam can represent a serious limitation of the present absorptiometric technique if deep test sections are used and strong concentration gradients are present. In theory, however, the refraction error could be corrected through

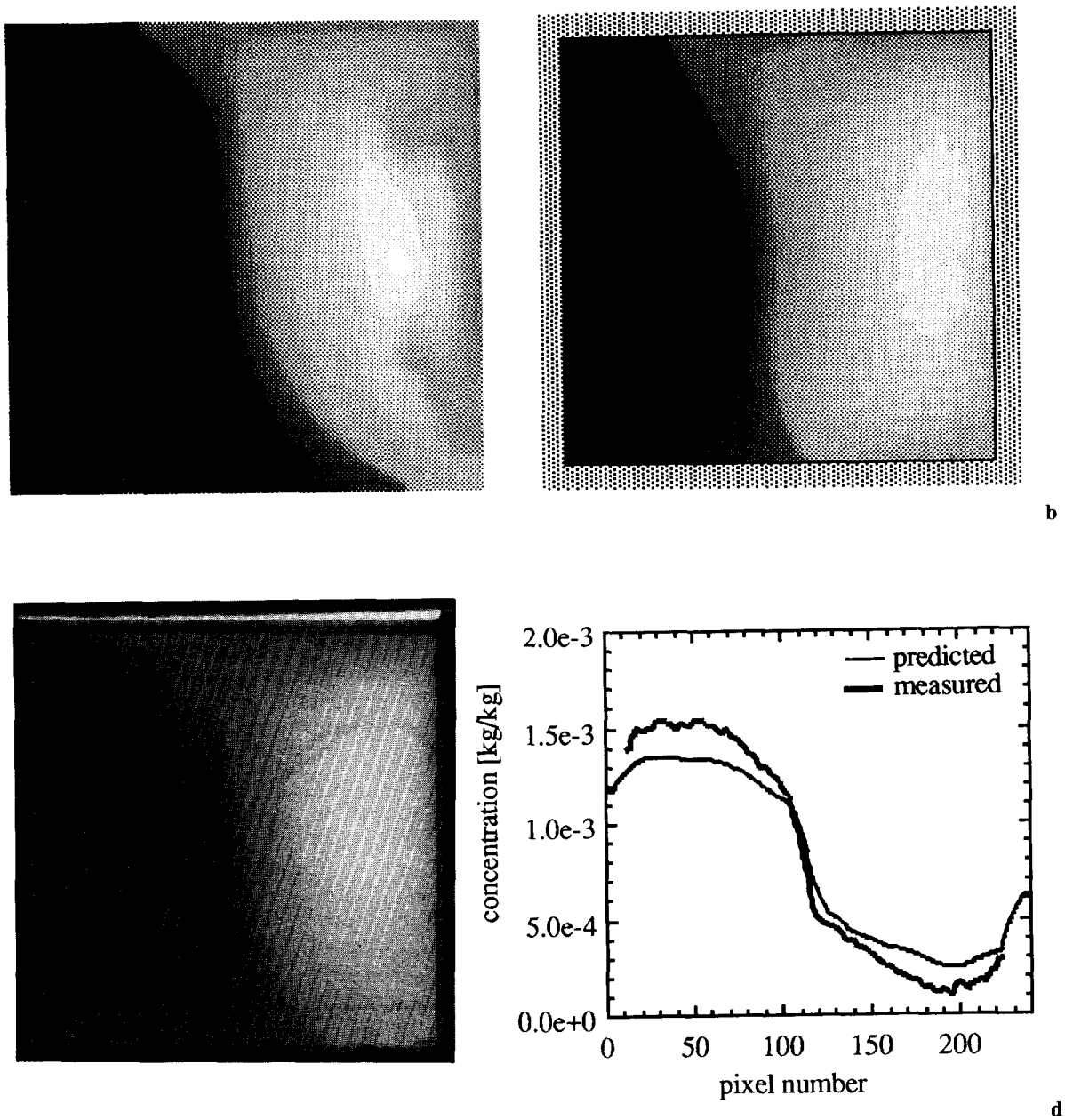

Figure 10. Results of the double-diffusive experiment at $t = 4$ h 34 min. (*a*) Predicted concentration field. (*b*) Measured concentration field. (*c*) Photograph. (*d*) Comparison of measured and predicted horizontal concentration profiles at the cell midsection.

mathematical manipulations of the measured intensity field. The accuracy and resolution could be somewhat enhanced by further flattening the incident light intensity distribution and by improving the systems for reducing the speckle effect and correcting for light intensity fluctuations. The technique could also be extended to measuring wider concentration ranges and/or multiple species concentrations by the simultaneous use of several laser light wavelengths or by combining it with other optical methods (such as interferometry).

The work reported in this paper was supported, in part, by the National Science Foundation under grants CBT-8808888 and CTS-8957149 and by a University of Iowa/NIH Biomedical Seed Grant. We thank Mr. C. Fan for his assistance with the numerical simulations.

NOMENCLATURE

C	concentration, kg/kg
I	light intensity, arbitrary units
Le	Lewis number [12], dimensionless
N	stability number [12], dimensionless
Ra	Darcy–Rayleigh number [12], dimensionless
t	time, s or min

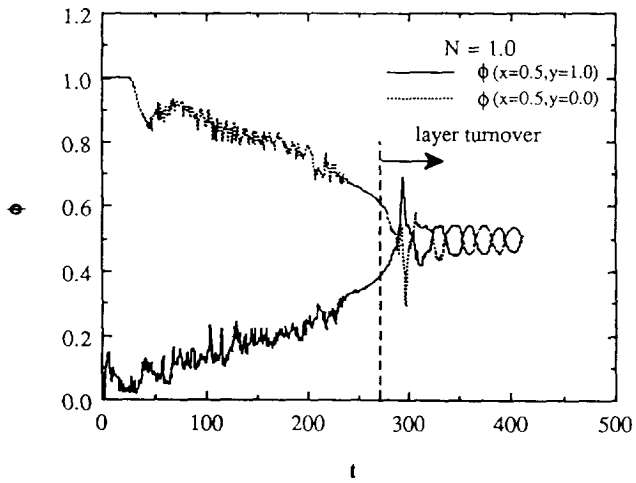

Figure 11. Predicted evolution of the dimensionless concentration at two points in the test cell. (From Ref. 12.)

Greek Symbols

α absorption coefficient, dimensionless
λ wavelength, m
σ thermal capacitance ratio [12], dimensionless
ϕ concentration [12], dimensionless

Subscripts

0 incident

REFERENCES

1. Mowbray, D. E., The Use of Schlieren and Shadowgraph Techniques in the Study of Flow Patterns in Density Stratified Liquids, *J. Fluid Mech.* **27,** 595–608, 1967.
2. Bergman, T. L., Munoz, D. R., Incropera, F. P., and Viskanta, R., Measurement of Salinity Distributions in Salt-Stratified, Double-Diffusive Systems by Optical Deflectometry, *Rev. Sci. Instr.* **57,** 2538–2542, 1986.
3. McCay, M. H., McCay, T. D., and Smith, L. M., Solidification Studies Using a Confocal Optical Signal Processor, *Appl. Opt.* **29,** 699–703, 1990.
4. Bedarida, R., Development of Holographic Interferometry Applied to Crystal Growth from Solution, *J. Crystal Growth* **79,** 43–49, 1986.
5. Ecker, A., A Two Wavelength Holographic Technique for Simultaneous Measurement of Temperature and Concentration During the Solidification of Two Component Systems, presented at AIAA 25th Aerospace Science Meeting, Reno, 1987.
6. Ruddick, B. R., The "Colour Polarigraph"—A Simple Method for Determining the Two-Dimensional Distribution of Sugar Concentration, *J. Fluid Mech.* **109,** 277–282, 1981.
7. Paul, T. R., and Bergman, T. L., Quantitative Measurement of Liquid Phase Species Distributions Using Optical Polarigraphy, presented at the National Heat Transfer Conference, Minneapolis, ASME Paper No. 91-HT-39, 1991.
8. Kazmierczak, M., and Poulikakos, D., An Optical Technique for the In-Situ Measurement of Species Concentration in Double Diffusive Convection, *Int. Commun. Heat Mass Transfer* **14,** 3–10, 1987.
9. Gau, C., and Wu, K. H., A Nonintrusive Technique for Concentration Distribution Measurement in Enclosures, *Exp. Heat Transfer* **2,** 215–226, 1989.
10. Körber, C., Scheive, M. W., and Wollhöver, K., Solute Polarization During Planar Freezing of Aqueous Salt Solutions, *Int. J. Heat Mass Transfer* **26,** 1241–1253, 1982.
11. Kourosh, S., Diller, K. R., and Crawford, M. E., Microscopic Study of Coupled Heat Mass Transport During Unidirectional Solidification of Binary Solutions. Part II. Mass Transfer Analysis, *Int. J. Heat Mass Transfer* **33,** 39–53, 1990.
12. Beckermann, C., Fan, C., and Mihailovic, J., Numerical Simulations of Double-Diffusive Convection in a Hele-Shaw Cell, *Int. Video J. Eng. Res.* **1,** 71–82, 1991.
13. Hartline, B. K., and Lister, C. R. B., Thermal Convection in a Hele-Shaw Cell, *J. Fluid Mech.* **79,** 379–389, 1977.
14. Ullmann, E., Experimentelle Beiträge zur Kenntnis der Diffusion in Lösungen, *Z. Physik* **41,** 301–317, 1926.
15. NRC, *International Critical Tables*, 1 and 5, National Research Council, New York, 1933.
16. Mihailovic, J., Development of Optical Two-Dimensional Species Concentration Measurement Technique for Binary Liquid Solutions, M.S.M.E. Thesis, Dept. Mechanical Engineering, Univ. Iowa, Iowa City, IA, 1993.

Received February 16, 1994; revised June 30, 1994